Hydrothermal synthesis and structures of organic-inorganic hybrid solids based on arsenic-vanadate building blocks

Yan-Fei Qi[a]; Yang-gang Li[a]; Enbo Wang[a]; Dong-rong Xiao[a]; Jin Hua[a]

[a] Department of Chemistry, Institute of Polyoxometalate Chemistry, Northeast Normal University, Jilin, P.R. China

PLEASE SCROLL DOWN FOR ARTICLE

Taylor & Francis
Taylor & Francis Group

Hydrothermal synthesis and structures of organic–inorganic hybrid solids based on arsenic-vanadate building blocks

YAN-FEI QI, YANG-GANG LI, ENBO WANG*,
DONG-RONG XIAO and JIN HUA

Department of Chemistry, Institute of Polyoxometalate Chemistry,
Northeast Normal University, Changchun, Jilin, 130024, P.R. China

Four novel organic–inorganic hybrid arsenic-vanadate complexes, $[Cu(phen)][(As^VO_4)(V^V_3O_7)(H_2O)]$ (**1**), $[Cu(en)_2]_2[As_8V_{14}O_{42}(H_2O)] \cdot 2.5H_2O$ (**2**), $[M(1,10\text{-phen})_3]_2[As_8V_{14}O_{42}(H_2O)_{0.5}] \cdot 0.5H_2O$ (M = Mn, **3**, Cd, **4**) (1,10-phen = 1,10-phenanthroline) have been hydrothermally synthesized for the first time and characterized by elemental analyses, XPS spectra, EPR spectra, IR spectra, TG analyses and single crystal X-ray diffraction. The structure of compound **1** consists of arsenic vanadate ribbons coordinated by the $[Cu(phen)]^{2+}$ complex, while compounds **2** to **4** possess a spherical $[As_8^{III}V_{14}^{IV}O_{42}]^{4-}$ cage with H_2O molecules encapsulated. The unexpected preparation **1** and the synthesis of compounds **2** to **4** on the basis of same polyoxoanion structures show that the pH value of the reaction plays a crucial role in controlling the basic architectures.

Keywords: Arsenic-vanadium; Building block; Hydrothermal synthesis; Organic–inorganic hybrid; Crystal Structure

1. Introduction

Interest in organic–inorganic hybrid polyoxometalates arises because of their enormous variety of structural topologies and potential applications in catalysis, conductivity, magnetochemistry and material science [1–4]. One approach employs various well characterized polyoxometalates as molecular building blocks bridged or supported by a transition metal complex to produce new families of organic–inorganic hybrid polyoxometalates, which exhibit interesting multi-dimensional frameworks and have fascinating properties from combining the unique characteristics of the organic and inorganic components [5, 6]. Based on this strategy, a large variety of organic–inorganic hybrid materials belonging to the {MxLy/V/O} or {MxLy/V/P/O} system (M = transition metal, L = organic ligand) have been isolated [7]. Compared with the rich structural chemistry in the V–P–O system, limited studies have been made on the V–As–O system. Studies have concentrated on discrete arsenic–vanadium clusters and anionic porous skeletons, such as $\{As^{III}_8V^{IV}_{14}O_{42}\}^{4-}$ (n = 3, 4) and MVOAsO$_4$

(M = Na, Li, NH_4) [8, 9]. More recently, some 2D layer-like and 3D porous V–As–O structures, such as [$H_2NC_4H_8NH_2$] [$(VO)_2(HAsO_4)_2(H_2AsO_4)_2$] and [$AsV_8^{IV}V_2^{V}O_{26}(H_2O)$]·$8H_2O$ have been prepared by hydrothermal techniques and organic templates [10, 11]. However, the V–As–O system as one of the most important subclasses of polyoxovanadates combined with a transition metal complex has been unexplored [12]. We are interested in mixed vanadium–arsenic polyoxoanion coordination abilities and quite recently successfully synthesized two new compounds of unprecedented structures composed of vanadium-arsenic-oxide and transition metal organic complexes [13, 14]. Herein, we reported the hydrothermal synthesis and crystal structures of four novel organic–inorganic hybrid arsenic vanadates in different pH solutions: [$Cu(phen)$][($As^{V}O_4$)($V^{V}_3O_7$)(H_2O)] (**1**), [$Cu(en)_2$]$_2$[$As^{III}_8V^{IV}_{14}O_{42}(H_2O)$]· $2.5H_2O$ (**2**), [$M(1,10\text{-phen})_3$]$_2$[$As^{III}_8V^{IV}_{14}O_{42}(H_2O)_{0.5}$]·$0.5H_2O$ (M = Mn, **3**, Cd, **4**) (1,10-phen = 1,10-phenanthroline). Compound **1** contains unprecedented $V_6O_{20}(H_2O)_2$ building blocks connected with AsO_4 to form a ribbon which is decorated by [$Cu(phen)$]$^{2+}$ fragments. The structure of compound **2** is a undee chain constructed from [$As_8^{III}V_{14}^{IV}O_{42}$] anion clusters and [$Cu(en)_2$]$^{2+}$ complexes. Compounds **3** and **4** possess a [$As_8^{III}V_{14}^{IV}O_{42}$] cage polyoxoanion and transition metal complex cations assembled through electrostatic interaction. In addition, hydrogen bonds and π–π interactions contribute to the building of these architectures. Furthermore, the syntheses of these new organic–inorganic arsenic–vanadium derivatives enrich the modifying chemistry of arsenic vanadate and also provides more information for the assembly process.

2. Experimental

2.1. *Synthesis and characterization*

All chemicals were commercially purchased and used without further purification. elemental analyses (C, H and N) were performed on a Perkin-Elmer 2400 CHN elemental analyzer. Mn, Cd, Cu, As and V were determined by a Leaman inductively coupled plasma (ICP) spectrometer. XPS analysis was performed on a VG ESCALABMK II spectrometer with a Mg-Kα (1253.6 eV) achromatic X-ray source. The vacuum inside the analysis chamber was maintained at 6.2×10^{-6} Pa during the analysis. IR spectra were recorded in the range of 400–4000 cm^{-1} on an Alpha Centaurt FT/IR spectrophotometer using KBr pellets. EPR spectra were recorded on a Japanese JES-FE3AX spectrometer at 293 K. TG analyses were performed on a Perkin-Elmer TGA7 instrument in flowing N_2 with a heating rate of 10°C min^{-1}.

2.2. *Synthesis of [Cu(phen)][($As^{V}O_4$)($V^{V}_3O_7$)(H_2O)] (1)*

Compound **1** was hydrothermally synthesized under autogenous pressure. A mixture of NH_4VO_3 (0.5 mmol), As_2O_3 (0.5 mmol), $CuCl_2 \cdot 2H_2O$ (0.5 mmol), 1,10-phen (0.3 mmol), HNO_3 (0.1 mL) and H_2O (5 mL) was mixed and stirred for 30 min in air. The mixture was sealed in a 15 mL Teflon-lined autoclave and heated at 160°C for 7 days. Then the autoclave was cooled at 10°C h^{-1} to room temperature. The resulting

green block crystals of **1** were filtered off, washed with distilled water, and dried at ambient temperature (yield: ca 22.7% based on V). Elemental analyses of the green crystals are consistent with the stoichiometry of $C_{12}H_{10}AsCuN_2O_{12}V_3$. The elemental analyses found: C, 22.57; H, 1.47; N, 4.38; V, 21.21; As, 11.54; Cu, 9.37%; Calcd for $C_{12}H_{10}AsCuN_2O_{12}V_3$: C, 21.66; H, 1.51; N, 4.21; V, 22.96; As, 11.26; Cu, 9.55%. IR spectrum (cm^{-1}): 3058(m), 1631(w), 1606(w), 1583(m), 1518(s), 1425(s), 1340(w), 1318(w), 1223(w), 1143(w), 1108(w), 977(s), 953(s), 938(s), 911(s), 839(s), 758(s), 739(s), 718(s), 665(s), 596(s), 518(s), 431(m), 405(m).

2.3. *Synthesis of [Cu(en)$_2$]$_2$[As$_8$V$_{14}$O$_{42}$(H$_2$O)] · 2.5H$_2$O (2)*

A mixture of NH_4VO_3 (0.5 mmol), As_2O_3 (0.5 mmol), $CuCl_2 \cdot 2H_2O$ (0.5 mmol), en (0.1 mL), HNO_3 (0.13 mL) and H_2O (5 mL) was mixed and stirred for 30 min in air. The mixture was sealed in a 15 mL Teflon-lined autoclave and heated at 160°C for 7 days. Then the autoclave was cooled at 10°C h^{-1} to room temperature. The resulting brown block crystals of **2** were filtered off, washed with distilled water, and dried at ambient temperature (yield: ca 32.72% based on V). Elemental analyses of the green crystals are consistent with the stoichiometry $C_{32}H_{84}As_{32}Cu_8N_{32}O_{182}V_{56}$. The elemental analyses found: H, 0.82; C, 4.11; N, 4.62; V, 29.81; Cu, 5.36; As, 25.11%; Calcd for $C_{32}H_{84}As_{32}Cu_8N_{32}O_{182}V_{56}$: H, 0.88; C, 4.01; N, 4.67; V, 29.75; Cu, 5.30; As, 25.01%. IR spectrum (cm^{-1}): 3468(m), 3241(m), 3139(w), 2951(w), 1624(w), 1587(m), 1368(m), 1047(m), 983(s), 758(m), 702(s), 622(w), 537(w), 452(w).

2.4. *Synthesis of [Mn(phen)$_3$]$_2$[As$_8$V$_{14}$O$_{42}$(H$_2$O)$_{0.5}$] · 0.5H$_2$O (3)*

A mixture of NH_4VO_3 (0.5 mmol), As_2O_3 (0.5 mmol), $KMnO_4$ (0.5 mmol), 1,10-phen (0.3 mmol) and H_2O (5 mL) was mixed and stirred for 30 min in air. The mixture was sealed in a 15 mL Teflon-lined autoclave and heated at 160°C for 7 days. Then the autoclave was cooled at 10°C h^{-1} to room temperature. The resulting green block crystals of **3** were filtered off, washed with distilled water, and dried at ambient temperature (yield: ca 10% based on V). Elemental analyses of the brown crystals are consistent with the stoichiometry $C_{72}H_{50}As_8Mn_2N_{12}O_{43}V_{14}$. The elemental analyses found: C, 27.17; H, 1.45; N, 5.34; V, 22.46; As, 18.69; Mn, 3.39%; Calcd for $C_{72}H_{50}As_8Mn_2N_{12}O_{43}V_{14}$: C, 27.08; H, 1.58; N, 5.26; V, 22.33; As, 18.77; Mn, 3.44%. IR spectrum (cm^{-1}): 3448(m), 3052(w), 1628(s), 1579(m), 1522(s), 1421(s), 1340(w), 1144(w), 1092(w), 994(s), 765(m), 716(s), 635(s), 548(m), 463(m).

2.5. *Synthesis of [Cd(1,10-phen)$_3$]$_2$[As$_8$V$_{14}$O$_{42}$(H$_2$O)$_{0.5}$] · 0.5H$_2$O (4)*

$NaVO_3 \cdot 2H_2O$ (0.782 mmol), As_2O_3 (0.611 mmol), $Cd(CH_3COO)_2$ (1.436 mmol), 1,10-phen (0.3 mmol) were mixed in a 7 mL NaAc/HAc buffer (pH = 4.8) and stirred for 30 min in air. The mixture was sealed in a 15 mL Teflon-lined autoclave and heated at 175°C for 5 days. Then the autoclave was cooled at 10°C h^{-1} to room temperature. The resulting black block crystals **4** were filtered off, washed with distilled water, and dried at ambient temperature (yield: ca 50.2% based on V). Elemental analyses of the black

crystals are consistent with the stoichiometry $C_{72}H_{50}As_8Cd_2N_{12}O_{43}V_{14}$. The elemental analyses found: C, 26.57; H, 1.47; N, 5.28; V, 21.21; As, 18.34; Cd, 6.37%; Calcd for $C_{72}H_{50}As_8Cd_2N_{12}O_{43}V_{14}$: C, 26.14; H, 1.52; N, 5.08; V, 21.56; As, 18.12; Cd, 6.79%. IR spectrum (cm^{-1}): 3440(m), 3063(w), 1613(s), 1591(m), 1521(s), 1424(s), 1338(w), 1142(w), 1090(w), 998(s), 763(m), 716(s), 632(s), 553(m), 461(m).

When $Cd(CH_3COO)_2$ was substituted by $Ni(CH_3COO)_2$ or $Co(CH_3COO)_2$ while the other reaction conditions remained the same, dark green block crystals of **5** [Ni(1,10-phen)$_3$]$_2$[As$_8$V$_{14}$O$_{42}$(H$_2$O)$_{0.5}$]$\cdot$1.5H$_2$O (45.2% yield based on V) and dark red block crystals of **6** [Co(1,10-phen)$_3$]$_2$[As$_8$V$_{14}$O$_{42}$(H$_2$O)$_{0.5}$]$\cdot$1.5H$_2$O (33% yield based on V) were obtained. Elemental analyses found for **5** $C_{72}H_{52}As_8N_{12}Ni_2O_{44}V_{14}$: H, 1.67; C, 26.80; N, 5.28; V, 22.21; Ni, 3.59; As, 18.69%. Calcd for $C_{72}H_{52}As_8N_{12}Ni_2O_{44}V_{14}$: H, 1.63; C, 26.86; N, 5.22; V, 22.15; Ni, 3.65; As, 18.62%. Elemental analyses found for **6** $C_{72}H_{52}As_8Co_2N_{12}O_{44}V_{14}$: H, 1.68; C, 26.80; N, 5.29; V, 22.23; As, 18.58; Co, 3.69%; Calcd for $C_{72}H_{52}As_8N_{12}Co_2O_{44}V_{14}$: H, 1.63; C, 26.86; N, 5.22; V, 22.15; As, 18.62; Co, 3.66%. IR spectrum (cm^{-1}) for **5**: 3454(m), 1622(w), 1581(m), 1514(m), 1430(s), 1146(w), 1108(w), 1000(s), 769(m), 715(s), 630(w), 553(w), 469(w). IR spectrum (cm^{-1}) for **6**: 3441(m), 1627(w), 1521(m), 1424(s), 1149(w), 1103(w), 998(s), 763(m), 716(s), 632(w), 560(w), 467(w).

When $Cd(CH_3COO)_2$ was substituted by $Mn(CH_3COO)_2\cdot 4H_2O$ or $Zn(CH_3COO)_2\cdot 2H_2O$ with the same synthetic conditions, brown crystals of **3** and dark crystals of **7** were obtained. The IR spectrum of **7** exhibits similar characteristic peaks as compounds **3**, **4**, **5** and **6**. However, owing to the poor quality of the crystals, no precise structure was determined by single crystal X-ray diffraction.

2.6. X-ray crystallography

The structures of compounds **1–6** were determined by single crystal X-ray diffraction. Data were collected on a Rigaku R-AXIS RAPID IP diffractometer with Mo-Kα ($\lambda = 0.71073$ Å) at 293 K. Empirical absorption correction (ψ scan) was applied. The structures were solved by the direct method and refined by full-matrix least squares on F^2 using the SHELXL-97 software [15]. For **1** and **2**, all of the non-hydrogen atoms were refined anisotropically. The hydrogen atoms of **1** were located from difference Fourier maps. Positions of the hydrogen atoms attached to carbon atoms of **2–4** were fixed at their ideal positions, and those attached to oxygen atoms were not located. For compounds **3** and **4**, in the cluster structure, four positions occupied by As$_2$O$_5$ dimers and four positions occupied by V atoms were disordered. The respective occupancies of those disordered As and V atoms were 0.5. Although the final residuals were relatively large, the molecular anion and transition-metal complexes were well behaved, and there were no unusual temperature factors or excursions of electron density in these regions of the structure. For compounds **5** and **6**, the refinement was complicated by disorder of the vanadium sites, the arsenic sites and the 1,10-phen ligands. Although the crystal structures of **5** and **6** could be roughly defined and further proved by elemental analyses and IR spectra, the final residuals of these compounds are too large to be reported. The summary of crystal data and structure refinements are provided in table S1.

A summary of crystal data and structure refinements for compounds **1–4** is provided in table 1. Ranges of selected bond lengths for **1–4** are listed in table 2.

Table 1. Crystal data and structure refinements for **1**–**4**.

Complex	1	2	3	4
Empirical formula	$C_{12}H_{10}AsCuN_2O_{12}V_3$	$C_{32}H_{84}As_{32}Cu_8N_{32}O_{182}V_{56}$	$C_{72}H_{50}As_8Mn_2N_{12}O_{43}V_{14}$	$C_{72}H_{50}As_8Cd_2N_{12}O_{43}V_{14}$
Formula weight	665.50	9587.53	3193.64	3308.56
Crystal system	Monoclinic	Monoclinic	Triclinic	Triclinic
Space group	$P2(1)/n$	$P2(1)/n$	$P\bar{1}$	$P\bar{1}$
a (Å)	12.630(3)	13.118(3)	11.416(2)	11.451(2)
b (Å)	7.535(5)	19.336(4)	15.796(3)	15.701(3)
c (Å)	19.518(4)	24.679(5)	15.967(3)	16.239(3)
α (°)	90	90	109.42(3)	109.39(3)
β (°)	93.73(3)	98.77(3)	92.07(3)	92.10(3)
γ (°)	90	90	104.43(3)	104.29(3)
Volume (Å^3)	1853.76	6187(2)	2607.69	2646.39
Z, D_c (Mg m^{-1})	4, 2.385	1, 2.617	1, 2.034	1, 2.076
Absorption coefficient (mm^{-1})	4.440	7.031	4.030	4.134
Reflections collected/unique	16699/4123 [$R_{(int)} = 0.0532$]	56472/14108 [$R_{(int)} = 0.0670$]	25340/11703 [$R(int) = 0.0520$]	20160/9168 [$R_{(int)} = 0.0585$]
Data/restraints/parameters	4123/0/320	14108/0/784	11703/4/745	9168/460/676
Goodness-of-fit on F^2	0.997	1.074	1.098	1.029
R_1 [a] [$I > 2\sigma(I)$]	0.0327	0.0488	0.0671	0.0629
wR_2 [b] [$I > 2\sigma(I)$]	0.0938	0.1675	0.2002	0.1756

[a] $R_1 = \sum ||F_o| - |F_c||/\sum |F_o|$; [b] $wR_2 = \sum [w(F_o^2 - F_c^2)^2]/\sum [w(F_o^2)^2]^{1/2}$.

Table 2. Some important bond lengths (Å) for compounds **1**–**4**.

Compound **1**

As(1)–O(4)	1.659(2)	As(1)–O(6)	1.699(2)
As(1)–O(12)	1.669(2)	As(1)–O(5)	1.724(2)
V(1)–O(2)	1.613(3)	V(2)–O(10)	1.691(3)
V(1)–O(1)	1.614(3)	V(2)–O(8)	1.838(2)
V(1)–O(10)#4	1.975(3)	V(2)–O(8)#2	1.974(2)
V(1)–O(4)	1.991(3)	V(2)–O(5)#3	2.013(2)
V(1)–O(3)	2.048(3)	Cu(1)–O(12)	1.940(3)
V(3)–O(7)	1.596(3)	Cu(1)–N(1)	1.988(3)
V(3)–O(11)#1	1.734(2)	Cu(1)–O(11)	2.000(2)
V(3)–O(6)	1.901(3)	Cu(1)–N(2)	2.013(3)
V(3)–O(8)	1.984(2)	Cu(1)–O(9)	2.348(2)
V(3)–O(5)#1	2.075(2)	V(2)–O(9)	1.619(2)

Compound **2**

As(6)–O(4)	1.768(4)	As(5)–O(7)	1.769(4)
As(6)–O(8)	1.772(4)	As(5)–O(21)	1.773(4)
As(6)–O(32)	1.778(4)	As(5)–O(26)	1.776(4)
As(4)–O(11)	1.771(4)	As(3)–O(9)	1.767(4)
As(4)–O(26)	1.779(4)	As(3)–O(33)	1.769(4)
As(4)–O(20)	1.791(4)	As(3)–O(39)	1.775(4)
As(2)–O(1)	1.751(4)	As(8)–O(13)	1.759(4)
As(2)–O(40)	1.770(4)	As(8)–O(32)	1.767(4)
As(2)–O(23)	1.777(4)	As(8)–O(27)	1.773(4)
As(7)–O(6)	1.764(4)	As(1)–O(19)	1.758(4)
As(7)–O(12)	1.768(4)	As(1)–O(2)	1.765(4)
As(7)–O(23)	1.788(4)	As(1)–O(33)	1.790(4)
V(14)–O(35)	1.592(5)	V(13)–O(38)	1.571(5)
V(14)–O(14)	1.944(4)	V(13)–O(21)	1.961(4)
V(14)–O(3)	1.963(4)	V(13)–O(20)	1.963(4)
V(14)–O(8)	2.004(4)	V(13)–O(27)	1.979(4)
V(14)–O(21)	2.019(4)	V(13)–O(8)	1.982(4)
V(12)–O(42)	1.604(5)	V(11)–O(31)	1.582(5)
V(12)–O(14)	1.924(4)	V(11)–O(9)	1.959(4)
V(12)–O(10)	1.938(4)	V(11)–O(2)	1.975(4)
V(12)–O(4)	1.979(4)	V(11)–O(40)	1.976(4)
V(12)–O(39)	1.991(4)	V(11)–O(6)	1.984(4)
V(10)–O(22)	1.598(4)	V(9)–O(28)	1.615(4)
V(10)–O(30)	1.922(4)	V(9)–O(16)	1.927(4)
V(10)–O(18)	1.923(4)	V(9)–O(18)	1.950(4)
V(10)–O(1)	1.978(4)	V(9)–O(13)	1.986(4)
V(10)–O(12)	1.994(4)	V(9)–O(1)	2.019(4)
Cu(1)–N(1)	1.988(6)	Cu(2)–N(6)	2.003(6)
Cu(1)–N(4)	1.993(6)	Cu(2)–N(8)	2.007(6)
Cu(1)–N(3)	1.999(6)	Cu(2)–N(7)	2.007(6)
Cu(1)–N(2)	2.016(6)	Cu(2)–N(5)	2.030(7)
V(8)–O(24)	1.594(4)	V(7)–O(36)	1.611(4)
V(8)–O(17)	1.942(4)	V(7)–O(3)	1.919(4)
V(8)–O(15)	1.942(4)	V(7)–O(15)	1.929(4)
V(8)–O(2)	2.003(5)	V(7)–O(7)	1.967(4)
V(8)–O(6)	2.003(4)	V(7)–O(19)	1.991(4)
V(6)–O(5)	1.607(4)	V(5)–O(29)	1.583(4)
V(6)–O(30)	1.926(4)	V(5)–O(10)	1.943(4)
V(6)–O(17)	1.936(4)	V(5)–O(16)	1.944(4)
V(6)–O(11)	1.995(4)	V(5)–O(9)	2.001(4)
V(6)–O(12)	2.003(4)	V(5)–O(40)	2.009(4)
V(4)–O(41)	1.610(4)	V(3)–O(34)	1.593(5)
V(4)–O(14)	1.910(4)	V(3)–O(30)	1.937(4)
V(4)–O(3)	1.933(4)	V(3)–O(18)	1.937(4)
V(4)–O(19)	1.990(4)	V(3)–O(20)	1.994(4)

(*Continued*)

Table 2. Continued.

V(4)–O(39)	1.992(4)	V(3)–O(27)	2.016(4)
V(2)–O(25)	1.606(4)	V(1)–O(37)	1.596(4)
V(2)–O(15)	1.930(4)	V(1)–O(16)	1.936(4)
V(2)–O(17)	1.948(4)	V(1)–O(10)	1.940(4)
V(2)–O(7)	1.966(4)	V(1)–O(4)	1.960(4)
V(2)–O(11)	1.977(4)	V(1)–O(13)	1.974(4)
Compound 3			
V(9)–O(18)	1.577(5)	V(8)–O(20)	1.595(4)
V(9)–O(6)#1	1.951(5)	V(8)–O(10)	1.947(5)
V(9)–O(8)	1.963(5)	V(8)–O(11)	1.952(5)
V(9)–O(7)#1	1.964(5)	V(8)–O(13)	1.961(5)
V(9)–O(15)	1.973(4)	V(8)–O(17)	1.971(5)
V(7)–O(12)	1.595(5)	V(6)–O(9)	1.588(5)
V(7)–O(16)	1.962(5)	V(6)–O(11)	1.946(5)
V(7)–O(14)	1.970(4)	V(6)–O(21)	1.953(5)
V(7)–O(21)#1	1.973(4)	V(6)–O(19)	1.959(5)
V(7)–O(19)#1	1.978(5)	V(6)–O(17)	1.966(5)
V(5)–O(4)	1.601(5)	V(4)–O(3)	1.438(6)
V(5)–O(14)	1.949(5)	V(4)–O(10)	1.836(5)
V(5)–O(10)	1.959(5)	V(4)–O(14)	1.863(5)
V(5)–O(16)	1.968(5)	V(4)–O(7)	2.137(5)
V(5)–O(13)	1.968(5)	V(4)–O(6)	2.154(6)
V(3)–O(5)	1.472(6)	V(2)–O(1)	1.362(7)
V(3)–O(13)	1.880(5)	V(2)–O(21)	1.835(5)
V(3)–O(16)	1.908(5)	V(2)–O(11)	1.945(5)
V(3)–O(15)	2.074(5)	V(2)–O(8)#1	2.096(5)
V(3)–O(8)	2.096(5)	V(2)–O(6)	2.155(5)
V(1)–O(2)	1.402(6)	As(2)–O(6)	1.696(5)
V(1)–O(17)	1.857(5)	As(2)–O(11)	1.881(5)
V(1)–O(19)	1.961(5)	As(2)–O(1)	1.913(8)
V(1)–O(15)	2.081(5)	As(8)–O(7)	1.749(5)
V(1)–O(7)#1	2.143(5)	As(8)–O(19)#1	1.878(5)
As(6)–O(8)	1.680(5)	As(8)–O(2)#1	1.887(7)
As(6)–O(1)#1	1.783(5)	As(7)–O(7)	1.634(5)
As(6)–O(21)#1	1.877(5)	As(7)–O(3)	1.901(6)
As(4)–O(15)	1.714(4)	As(7)–O(14)	1.918(5)
As(4)–O(2)	1.787(6)	As(1)–O(6)	1.679(5)
As(4)–O(17)	1.854(5)	As(1)–O(3)	1.822(6)
As(5)–O(8)	1.749(5)	As(1)–O(10)	1.944(5)
As(5)–O(5)	1.846(6)	As(3)–O(15)	1.735(4)
As(5)–O(16)	1.921(5)	As(3)–O(5)	1.808(6)
Mn(1)–N(6)	2.229(6)	As(3)–O(13)	1.920(5)
Mn(1)–N(2)	2.232(6)	Mn(1)–N(5)	2.236(7)
Mn(1)–N(4)	2.233(7)	Mn(1)–N(3)	2.250(8)
Mn(1)–N(1)	2.272(6)		
Compound 4			
As(1)–O(1)	1.698(5)	As(5)–O(3)	1.721(5)
As(1)–O(20)	1.789(7)	As(5)–O(9)#1	1.877(5)
As(1)–O(8)	1.880(5)	As(5)–O(26)#1	1.909(8)
As(2)–O(2)	1.709(5)	As(6)–O(4)	1.702(5)
As(2)–O(7)	1.872(5)	As(6)–O(26)#1	1.804(7)
As(2)–O(20)	1.930(8)	As(6)–O(6)#1	1.856(5)
As(3)–O(2)	1.674(6)	As(7)–O(4)	1.737(6)
As(3)–O(27)	1.805(7)	As(7)–O(11)	1.805(7)
As(3)–O(21)	1.946(6)	As(7)–O(18)#1	1.943(6)
As(4)–O(3)	1.644(6)	As(8)–O(1)	1.742(5)
As(4)–O(27)	1.905(7)	As(8)–O(11)	1.859(7)

(*Continued*)

Table 2.   Continued.

As(4)–O(22)#1	1.933(6)	As(8)–O(23)	1.936(6)
V(1)–O(5)	1.580(5)	V(2)–O(11)	1.492(6)
V(1)–O(2)	1.957(5)	V(2)–O(18)#1	1.866(5)
V(1)–O(1)	1.960(5)	V(2)–O(23)	1.899(6)
V(1)–O(4)	1.968(5)	V(2)–O(4)	2.095(6)
V(1)–O(3)	1.970(5)	V(2)–O(1)	2.096(6)
V(3)–O(20)	1.395(7)	V(4)–O(27)	1.441(7)
V(3)–O(8)	1.868(6)	V(4)–O(21)	1.822(6)
V(3)–O(7)	1.943(5)	V(4)–O(22)#1	1.881(5)
V(3)–O(1)	2.093(6)	V(4)–O(2)	2.139(6)
V(3)–O(2)	2.145(6)	V(4)–O(3)	2.161(6)
V(5)–O(24)	1.594(6)	V(6)–O(10)	1.599(5)
V(5)–O(22)	1.954(5)	V(6)–O(8)	1.949(5)
V(5)–O(23)	1.970(6)	V(6)–O(9)	1.952(6)
V(5)–O(8)	1.975(5)	V(6)–O(7)	1.952(6)
V(5)–O(9)	1.976(6)	V(6)–O(6)	1.971(5)
V(7)–O(19)	1.594(5)	V(8)–O(25)	1.594(6)
V(7)–O(21)	1.958(6)	V(8)–O(23)	1.956(5)
V(7)–O(7)	1.959(5)	V(8)–O(21)#1	1.956(6)
V(7)–O(18)	1.966(5)	V(8)–O(22)	1.956(6)
V(7)–O(6)	1.967(6)	V(8)–O(18)#1	1.964(6)
V(9)–O(26)	1.412(7)	V(9)–O(4)#1	2.088(6)
V(9)–O(6)	1.874(6)	V(9)–O(3)#1	2.136(6)
V(9)–O(9)	1.946(6)	Cd1–N6	2.330(5)
Cd1–N1	2.339(5)	Cd1–N5	2.343(5)
Cd1–N4	2.344(6)	Cd1–N3	2.350(5)
Cd1–N2	2.391(5)		

Note: #1: −x, −y−2, −z#2: −x, −y−3, −z#3: x, y−1, z#4: x, y+1, z for compound 1.
#1: −x+2, −y, −z+1 for compound 3.
#1: #1 −x+1, −y+1, −z for compound 4.

3. Results and discussion

3.1. *Synthesis*

Hydrothermal reactions have proved to be an effective technique for preparation of numerous of solid-state oxides and organic–inorganic hybrid materials providing special reaction conditions in which different solubility problems are minimized. In a specific hydrothermal process, many factors can affect the formation and crystal growth of products, such as the type of initial reactants, starting concentrations, pH, reaction time and temperature. Aqueous chemistry of vanadium is very complex; it was anticipated that vanadate could form different building units under different pH ranges [16, 17]. In our case, the pH value of the reaction system was crucial important for the crystallization of products. Compounds **1** and **3** were both separated from the hydrothermal reactions of NH_4VO_3, As_2O_3, transition metal salt and 1,10-phen at 160°C for 6 days with difference in pH values of the initial reaction solutions. At low pH (ca 2), the V (V) and As (V) co-exist in the hydrothermal system and compound **1** was formed. At higher pH (ca 5), only the V (IV) and As (III) co-exist in the reaction to product **3**. Compound **3** can also crystallize in poor quality from another hydrothermal reaction mixture at approximately pH 4.5–5.0 in which compounds **4**, **5** and **6** were prepared. When the pH value of the reaction system was adjusted to about 7.0 by en, compound **2** was synthesized. There is no obvious difference of the starting organic
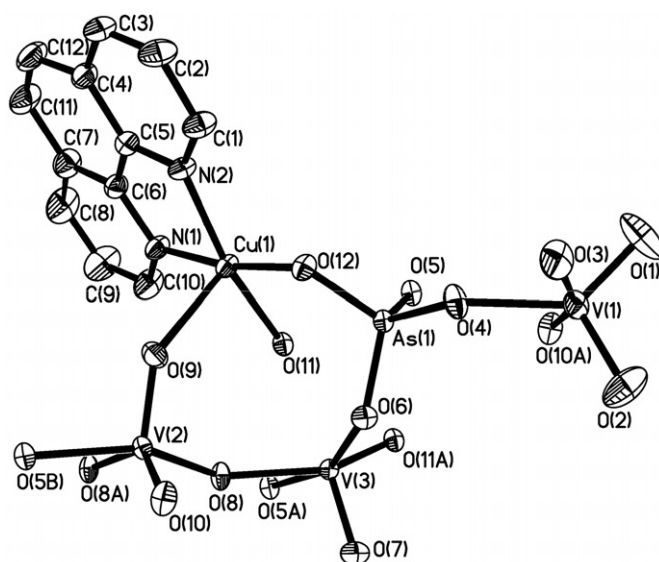
Figure 1. ORTEP drawing of compound **1** with thermal ellipsoids at 50% probability. H atoms are omitted for clarity. Symmetry of the atoms with code A and B: $-x$, $-2-y$, $-z$; x, $1+y$, z; $-x$, $-3-y$, $-z$; $-x$, $-1+y$, z.

ligand and transition metal in formation of the $[As^{III}_8 V^{IV}_{14} O_{42}]$ building block in compounds **2**–**6** at approximately pH 4.5–7. If the reaction solution pH is increased above 7, no crystalline phase was formed. In addition, the organonitrogen ligands are also very significant, functioning as a ligand bound to a secondary metal site, as a reductive agent or as an alkaline agent to adjust the pH value. The en molecule performs all three functions in **2**. Besides being a ligand, the 1,10-phen molecule in preparation of **3** takes a role as a reducing agent that cannot be proved clearly in the syntheses of compounds **4**–**6**.

3.2. Structure description

Single crystal X-ray diffraction analysis reveals that compound **1** consists of arsenic vanadate ribbons coordinated with the $[Cu(phen)]^{2+}$ complex. There are three crystallographically independent V atoms, one As atom and one Cu atom in this structure, as shown in figure 1. The V(1) sites possess a distorted trigonal bipyramidal $3+2$ geometry with the shorter vanadyl bonds (V1–O1, 1.614 Å; V1–O2, 1.613 Å) occupying two equatorial positions and the longer bonds (V1–O4, 1.991 Å) occupying one equatorial and two (V1–O3, 2.048 Å; V1–O10, 1.975 Å) axial positions. The V(2) and V(3) centers show a distorted $\{VO_5\}$ square pyramidal environment. The V(2) atom bonds five bridging oxygen atoms with V–O distances in the range of 1.619(2)–2.013(2) Å and O–V–O angles 72.43(9)–147.41(9)°. The V(3) site is defined by one terminal oxygen atom and four bridging oxygen atoms with V–O distances in the range of 1.596(3)–2.075(2) Å and O–V–O angles 70.92(9)–157.99(1)°. The Cu(II) site exhibits the common square pyramidal geometry coordinated with one oxygen atom of one

adjacent {AsO$_4$} tetrahedron, two oxygen atoms of two {VO$_5$} square pyramids and two nitrogen donors of phen group. The average Cu–N and Cu–O bond lengths are 2.00(8) and 2.09(6) Å, respectively. The O(N)–Cu–N(O) angles vary from 82.63(1) to 170.80(1)°. The As centers possess a {AsO$_4$} tetrahedral environment. The As–O distances are in the range of 1.659(2)–1.724(2) Å and O–As–O angles in the range of 106.47(1)–112.15(1)°.

An unusual structural feature is that **1** exhibits novel {As–V–O} inorganic ribbons based on the fundamental building units V$_6$O$_{20}$(H$_2$O)$_2$ ({V$_6$}unit) as shown in figure 2. In the {V$_6$} unit, four {VO$_5$} distorted square pyramids connect with each other by edge-sharing oxygen atoms to form an interesting *Z*-type tetra-vanadate with two apical oxygen atoms directed above the plane of the paper and the other two oxygen atoms directed below. The two {V(1A)O$_5$} and {V(1AA)O$_5$} distorted trigonal bipyramids connect with *Z*-type tetra-vanadate through two corner oxygen atoms O(10) and O(10A). Two adjacent {V6} units are held together by two corner-sharing AsO$_4$ tetrahedra through the bridged oxygen atoms (O(5), O(6) and O(4), and their equivalent atoms), to form the interesting ribbon. There are eight-membered {V$_2$As$_2$O$_4$} and six-membered {V$_2$AsO$_3$} rings in the inorganic ribbon. The [Cu(phen)]$^{2+}$ coordination complexes are grafted onto the arsenic vanadate ribbon. Each complex cation bonds to
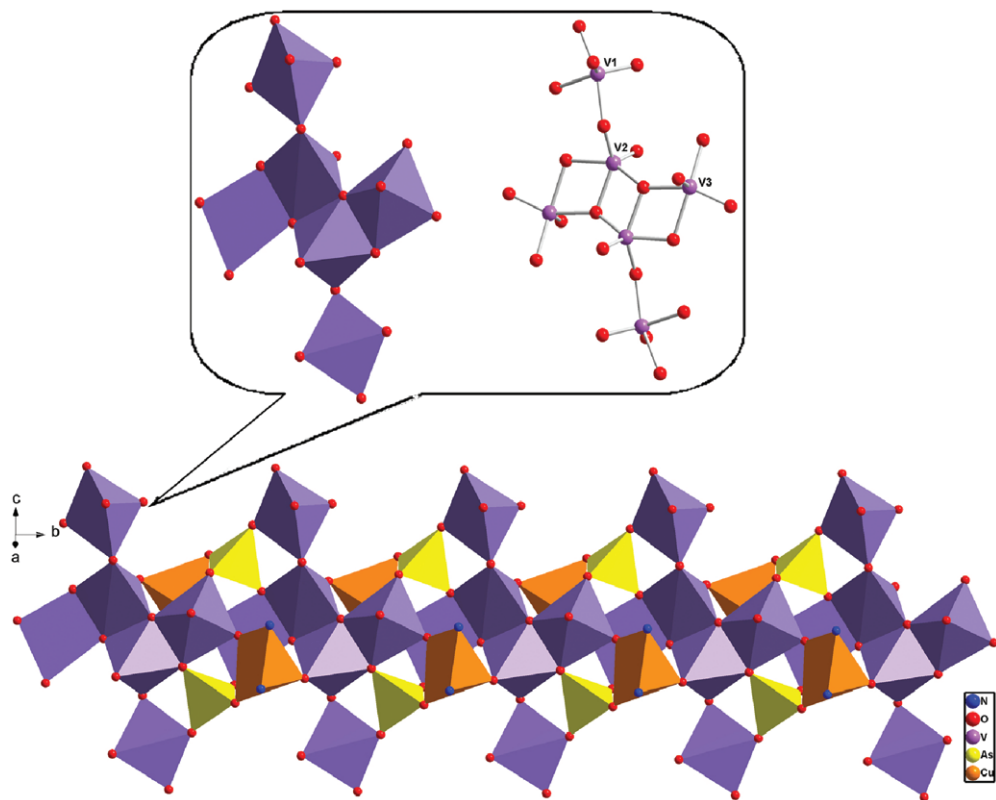

Figure 2.   The one-dimensional inorganic ribbon in **1**. A polyhedral representation and labelling scheme of the {V$_6$} building block.

one {AsO$_4$} tetrahedron and acts as bridge, linking with adjacent {V$_6$} units *via* two oxygen atoms on the {VO$_5$} units. In summary, the structure of **1** can be described as a one-dimensional ribbon constructed from V$_6$O$_{20}$(H$_2$O)$_2$ building blocks connected with {AsO$_4$} tetrahedrons and {CuO$_3$N$_2$} square pyramids. To our knowledge, only two vanadium arsenate compounds decorated with metal-organic complexes, [Cu(2,2′-bpy)](VO$_2$)(AsO$_4$) [14] and [Cu(phen)]$_2$[V^{IV}V$^V_4$As$^V_2$O$_{19}$]·0.5H$_2$O [13] have been reported. Compared with the two structures, the vanadium(V) centers exhibit different polyhedra and more complex coordination. No isolated vanadium oxide complex fragments existing in compound **1** are found in the above two examples. The aqua ligand bonded to the V centers is an active site, which may extend the one-dimensional structure into a high dimensional structure. The adjacent ribbons are packed together and exhibit an interesting three-dimensional supramolecular architecture *via* two types of supramolecular interactions. One is the significant hydrogen bonding interaction between hydrogen atoms of V1–O3 and oxygen atoms from the other ribbons. The typical hydrogen bonds are O(3)–H(3A)···O(1) 2.608 Å, and O(3)–H(3B)···O(12) 2.691 Å (see figure S1). The other is the weak aromatic π–π stacking interaction of the 1,10-phen groups between adjacent ribbons, the close contact distance between adjacent phen rings is 3.756 Å (see figure S2).

When the pH value of the reaction solution was changed, compounds **2** and **3** were isolated. Compound **4** synthesized in another reaction solution is isostructural with **3**. The structures of compounds **2** to **4** all contain the {As$^{III}_8$V$^{IV}_{14}$O$_{42}$} cluster as anions. As reported in the literature [18], the polyoxoanion could be regarded as a derivative of the Keggin analog {V$_{18}$O$_{42}$} cluster shell, which is built up from 14 VO$_5$ square pyramids and 8 AsO$_3$ triagonal pyramids, with half or one H$_2$O molecule at the center. Two AsO$_3$ groups are joined by an oxygen bridge to form an As$_2$O$_5$ moiety. Eight VO$_5$ square pyramids are held together to form a ring by edge-sharing oxygen atoms. In addition, another six vanadium oxygen square pyramids are divided into two groups, each group of VO$_5$ square pyramids share edges to form a trimer. The two trimers are on opposite sides of the ring and connected across the ring by sharing edges with two VO$_5$ square pyramids. The remaining four faces are capped by As$_2$O$_5$ units to give a total anion composition of [As$_8$V$_{14}$O$_{42}$]$^{4-}$. In the structure of the As$_8$V$_{14}$ cluster in **1**, eight VO$_5$ square pyramids are held together to form a ring, however, an interesting phenomenon is that the two As–V coronets on the opposite sides of the rings of **3** and **4** were disordered. As shown in figure 3(b), in each coronet, four positions occupied by As$_2$O$_5$ units are disordered over eight positions with free refined occupancy of 0.5 for each position to form a 16-member Latin Cross like ring. At the same time, four positions occupied by VO$_5$ square pyramids are also disordered over eight positions (V1, V2, V3, V4, V1A, V2A, V3A and V4A atoms in **3**; V2, V3, V4, V9, V2A, V3A, V4A and V9A in **4**) with free refined occupancy of 0.5 for each position. Because of the position disorder, the V–O distances are in the range of 1.362(7)–2.155(5) Å in **3** and 1.395(7)–2.161(6) Å in **4**. The As–O distances are in the range of 1.634(5)–1.944(5) Å in **3** and 1.644(6)–1.946(6) Å in **4**. The structures of the disordered As$_8$V$_{14}$ anion in **3** and **4** can also be described as a well-known {V$_{18}$O$_{42}$} rhombicuboctahedron encircled by two arsenic rings.

The structure of the [As$_8$V$_{14}$O$_{42}$(H$_2$O)] core in **2** is not disordered and identical to that reported for (N(CH$_3$)$_4$)$_4$[V$_{14}$As$_8$O$_{42}$(H$_2$O)], as shown in figure 3(a). There are fourteen crystallographically independent V atoms and eight As atoms in the unit. Each square-pyramidal V atom is defined by a terminal oxygen atom and four bridging
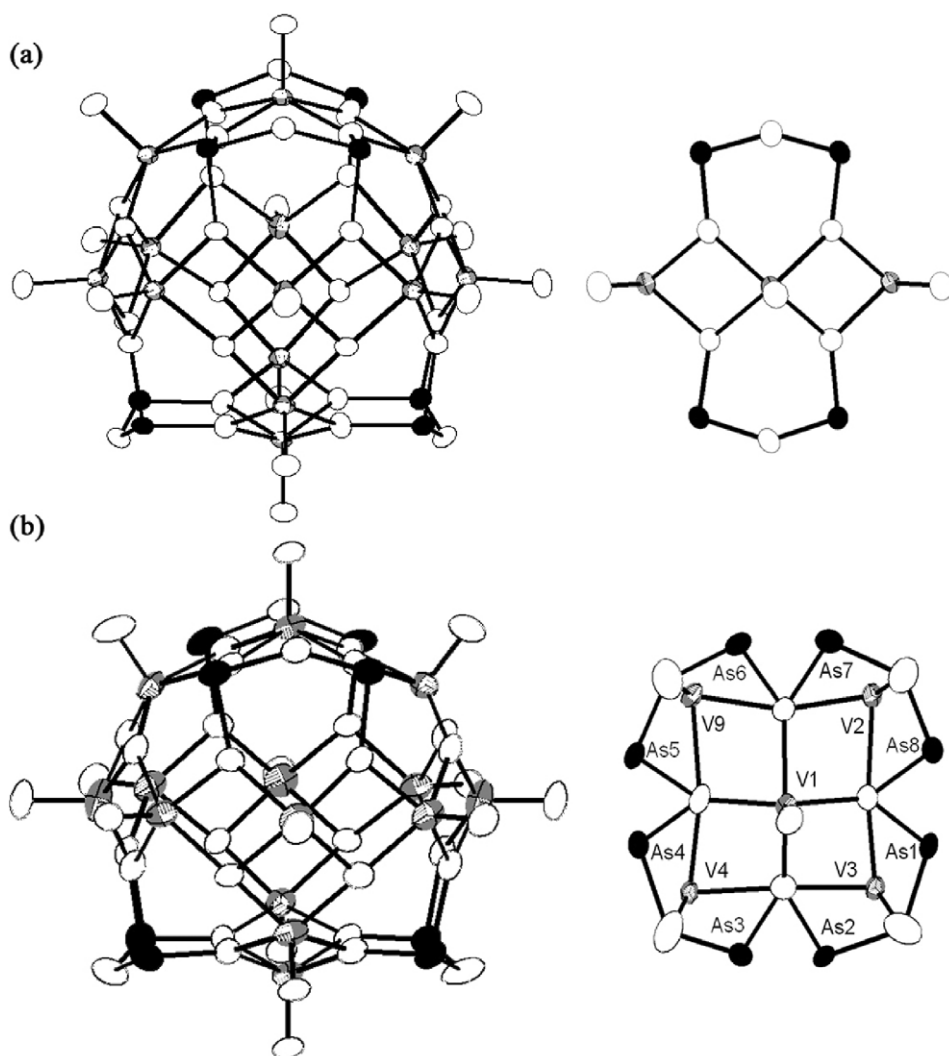
Figure 3. ORTEP drawing of the $[As^{III}_8V^{IV}_{14}O_{42}]$ shell and the coronet in the compounds **2** (a) and **3** (b) with thermal ellipsoids at 30% probability.

oxygen atoms with V–O bond lengths in the range of 2.019(4)–1.583(4) Å and O–V–O angles 75.5(3)–148.9(1)°. The As–O distances are from 1.751(4) to 1.791(4) Å and O–As–O angles are between 99.8(9) and 97.7(2)°. There are two crystallographic independent copper sites (Cu(1) and Cu(2)) in compound **2**. The copper sites exhibit a distorted octahedral coordination geometry which is defined by coordination from the ethylenediamine ligands (Cu(1)–N distance 1.988(6)–2.016(6) Å, Cu(2)–N distance 2.003(6)–2.030(7) Å) and two trans terminal oxygen atoms from two different decavanadate anions, and these copper atoms exhibit very weak interactions with the clusters (Cu(1)–O distances 2.732(4) and 2.796(0) Å; Cu(2)–O distances 2.647(4) and 2.699(8) Å). Four terminal oxygen atoms from alternate VO5 square pyramids on the eight member ring of one cluster coordinate to four bridging copper atoms, so each
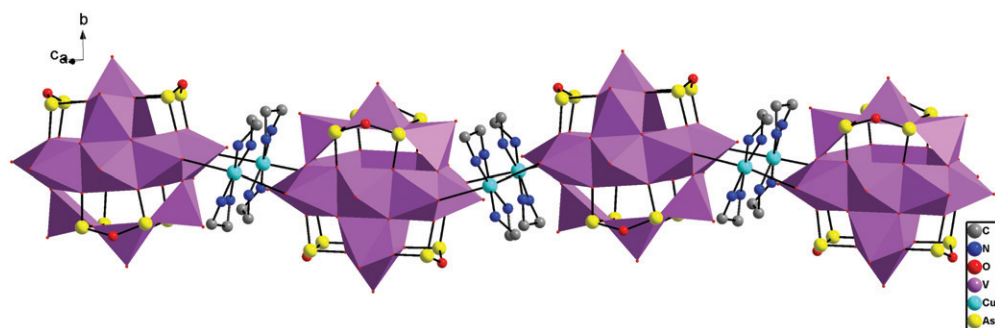
Figure 4. The one-dimensional undee chain structure of the compound **2**.

$[As^{III}_8V^{IV}_{14}O_{42}(H_2O)]^{4-}$ cluster is connected with the neighboring ones through the $[Cu(en)_2]^{2+}$ double bridge, alternatively, to form a undee chain structure, as shown in figure 4 and figure S3. The 1-D chains in compound **2** are arranged parallel to each other and further connect each other through hydrogen bonds (OW2$\cdots$O29 2.958 Å, OW2$\cdots$OW3A 2.964 Å, OW3$\cdots$OW5 2.953 Å, OW3$\cdots$O18 2.972 Å, OW4$\cdots$O31 2.964 Å, OW4$\cdots$O24 2.950 Å, OW4$\cdots$N2A 2.924 Å and OW5$\cdots$O35A 2.983 Å) to generate an interesting three-dimensional supermolecular structure, shown in figure S4.

The structures of compounds **3** and **4** contain discrete $[As^{III}_8V^{IV}_{14}O_{42}]^{4-}$ clusters, transition metal complex cations, and isolated water molecules. Each metal(II) site in **3** (M = Mn) and **4** (M = Cd) is coordinated with six nitrogen atoms in three 1,10-phen groups to form a chiral cation unit with M–N bond distances in the range of 1.929(4)–1.949(4) Å for **3**, 2.330(5)–2.391(5) Å for **4**, respectively. Four $[M(1,10\text{-phen})_3]^{2+}$ groups lie in the same plane. The polyoxoanions are located above and below this plane and are connected with the $[M(1,10\text{-phen})_3]^{2-}$ groups via electrostatic attraction, as shown in figure 5. Such role of secondary metal-ligands as an isolated charge-balancing cation appears to be a common characteristic of the hydrothermal chemistry of these organic–inorganic polyoxometalate derivatives. However, these classes of compounds are very rare in arsenic–vanadium clusters.

The bond valence sum calculations [19] give the average values of 5.1, 5.1, 4.8 and 5.0 for V1, V2, V3 and As, indicating that both V and As are in the +5 oxidation state in compound **1**. The XPS spectra of compound **1** in the energy regions of V_{2p} and As_{3d} show peaks at 516.6 and 44.9 eV, attributable to V^{5+} and As^{5+}, respectively (figure S7). The average BVS values for vanadium and arsenic are 4.34 and 3.14 in **2**, 4.56 and 2.81 in **3**, 4.40 and 2.85 in **4**, respectively, indicating that the oxidation state for each vanadium atom and each arsenic atom is +4 and +3 respectively. The EPR spectra of compounds **3** and **4** at room temperature exhibit the V^{4+} signal with $g = 1.9671$, $A = 600$G, and $g = 1.9599$, $A = 550$G (figures S16 and S17) respectively, consistent with the valence sum calculations.

3.3. *FT-IR spectroscopy and thermal analysis*

In the IR spectra, as shown from figures S8 to S11, vibration modes for v(V=O) and v(V–O–M) (M=V or As) are observed at 977, 953, 938, 911, 838, 758, 739, 718, 665,
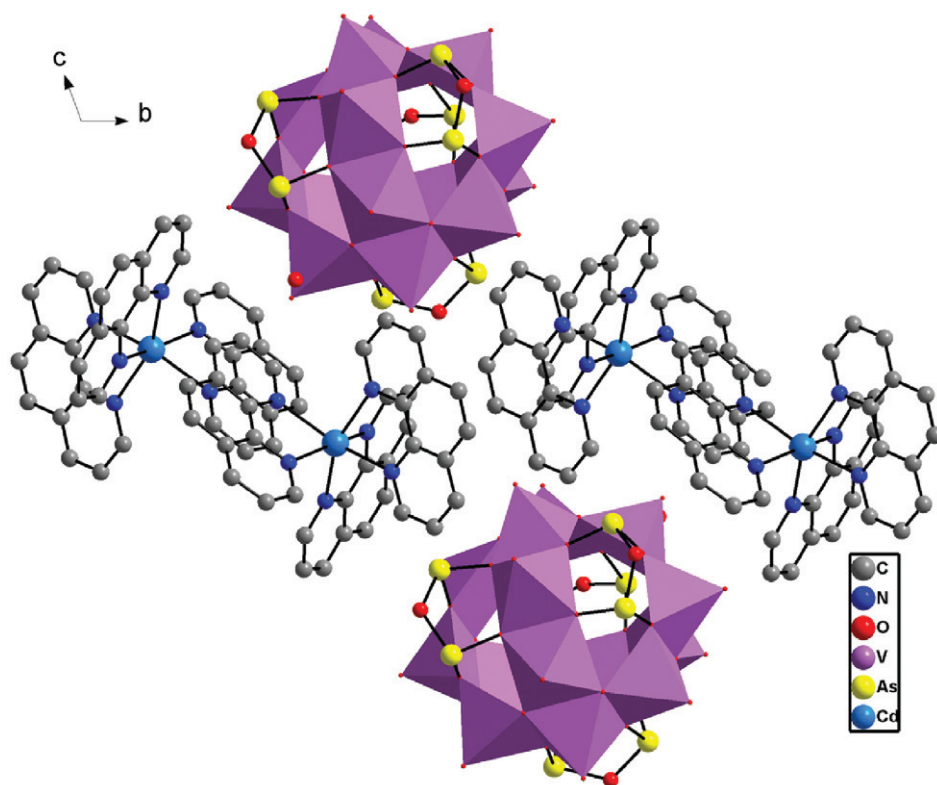
Figure 5.   View of crystal packing of compound **4** along *a*-axis.

596, 518, 431 and 405 cm^{-1}, **1**; 983, 758, 702, 622, 537 and 452 cm^{-1}, **2**; 994, 765, 716, 635, 548 and 463 cm^{-1}, **3**; 998, 763, 716, 632, 553 and 461 cm^{-1}, **4**; The characteristic absorption bands of organonitrogen ligands occur at 1583, 1518, 1425, 1143, 1108 cm^{-1}, **1**; 1047, 1368, 1587, 2951, 3139 and 3241 cm^{-1}, **2**; 1522, 1421, 1144, 1092 cm^{-1}, **3**; 1591, 1521, 1424, 1142, 1090 cm^{-1}, **4**; The IR data show that the $V^{IV}=O_{term}$ bands in compounds **3** and **4** are at higher energy than that in **2** and more similar to the $V=O_{term}$ reported in literature [18b].

The TG curves (see Supporting Information from figures S12 to S15) for compounds **1**–**4** also support their chemical compositions. All the weight losses of the six complexes are attributable to the loss of coordination water, the decomposition of organoamine ligands and the sublimation of As_2O_3. In the curve of compound **1**, the first weight loss is in the range of 301–342°C and the second weight loss at 345–596°C. The whole weight loss 53.30% is in agreement with the calculated value 55.08%. The sample does not lose weight at temperatures higher than 635°C. Three continuous weight losses at 45–529°C are observed in compound **2**. The whole weight loss of 47.39% is in agreement with the calculated value 44.93%. The sample does not lose weight at temperatures higher than 529°C. Compounds **3** and **4** have similar TG curves with three-weight losses at about 40–120°C, 345–413°C, 438–520°C, and the whole weight loss of 57.39%, **3** and 53.37%, **4** are in agreement with the calculated values

59.55%, **3** and 57.87%, **4**. The samples do not lose weight at temperatures higher than 507 and 519°C.

The redox behaviors of **1** and **4** were investigated by cyclic voltammetry in 1 M H_2SO_4, shown figure S18. A CHI 660 Electrochemical Workstation connected to a Digital-586 personal computer was used for control of the electrochemical measurements and for data collection. A conventional three-electrode system was used. The working electrodes were compounds **1** and **4** bulk-modified carbon paste electrodes, respectively. A SCE was used as reference electrode and Pt gauze as a counter electrode. In the potential range 2000 to −1500 mV, two redox peaks appear and the mean peak potentials $E_{1/2} = (E_{pa} + E_{pc})/2$ are 833(I) and −494(II) mV in compound **1**; 883(I) and −596(II) mV in compound **4**. The redox peaks I–I′ and II–II′ are attributed to V(V)/V(IV), As(V)/As(III), respectively.

4. Conclusions

In this article, we have prepared and structurally characterized four arsenic-vanadate complexes. The successful synthesis of [Cu(phen)](As^VO_4)($V^V_3O_7$)(H_2O) which contains a new vanadium oxide building blocks provides another model for the {MxLy/V/As/O} (M = transition metal, L = organic ligand) system. Changing the pH, the organic–inorganic complexes containing arsenic-vanadate cluster [$As^{III}_8V^{IV}_{14}$] were obtained. As for compounds **2–4**, the pH value of the reaction system is very important. Furthermore, the successful syntheses of these six novel arsenic–vanadium derivatives prove again the advantages of hydrothermal techniques in designing new kinds of structural organic–inorganic hybrid solids. Also, utilizing this inorganic arsenic–vanadium as building block to prepare more favorable models for material science may be possible.

Supplementary material

Crystallographic data for the structural analysis have been deposited with the Cambridge Crystallographic Data Centre, CCDC reference numbers 290616, 293712, 295521 and 295522. These data can be obtained free of charge at www.ccdc.cam.ac.uk/conts/retrieving.html (or from the Cambridge Crystallographic Data Centre, 12, Union Road, Cambridge CB2 1EZ, UK; Fax: C44 1223/336 033; Email: deposit@ccdc.cam.ac.uk).

Acknowledgements

References

[1] (a) L.C.W. Baker, D.C. Glick. *Chem. Rev.*, **98**, 3 (1998); (b) P. Gouzerh, A. Proust. *Chem. Rev.*, **98**, 77 (1998).

[2] P.J. Hagrman, D. Hagrman, J. Zubieta. *Angew. Chem. Int. Ed.*, **38**, 2638 (1999).

[3] A.K. Cheetham, G. Férey, T. Loiscau. *Angew. Chem. Int. Ed.*, **38**, 3268 (1999).

[4] T. Chirayil, P.Y. Zavalij, M.S. Whittingham. *Chem. Mater.*, **10**, 2629 (1998).

[5] A. Müller, P. Kögerler. *Coord. Chem. Rev.*, **182**, 3 (1999).

[6] P.J. Hagrman, R.C. Finn, J. Zubieta. *Solid State Sci.*, **3**, 745 (2001).

[7] (a) Y.G. Li, E.B. Wang, H. Zhang, G.Y. Luan, C.W. Hu, N.H. Hu, H.Q. Jia. *J. Solid State Chem.*, **163**, 10 (2002); (b) Y. Lu, E.B. Wang, M. Yuan, G.Y. Luan, Y.G. Li. *J. Chem. Soc., Dalton Trans.*, 3029 (2002); (c) Z. Shi, S.H. Feng, S. Gao, L.R. Zhang, G.Y. Yang, J. Hua. *Angew. Chem. Int. Ed.*, **39**, 2325 (2000); (d) X.M. Zhang, M.L. Tong, X.M. Chen. *Chem. Commun.*, 1817 (2000); (e) R.L. LaDuuca, R.S. Rarig, J. Zubieta. *Inorg. Chem.*, **40**, 607 (2001).

[8] A. Müller, J. Döring. *Angew. Chem., Int. Ed.*, **27**, 1721 (1988).

[9] (a) A. Haddad, T. Jouini, Y. Piffard. *Eur. J. Solid State Inorg. Chem.*, **29**, 57 (1992); (b) J. Ganbicher, F. Orsini, T. Le Mercier, S. Llorente, A. Villesuzanne, M. Quarton. *J. Solid State Chem.*, **150**, 250 (2000).

[10] R.C. Haushalter, E. Wang, L.M. Meyer, S.S. Dhengra, M.E. Thompson, J. Zubieta. *Chem. Mater.*, **9**, 1463 (1994).

[11] (a) W.M. Bu, L. Ye, G.Y. Yang, M.C. Shao, Y.G. Fan, J.Q. Xu. *Chem. Commun.*, 1279 (2000); (b) Y.N. Zhao, Q.S. Liu, Y.F. Li, X.M. Chen, Z.H. Mai. *J. Mater. Chem.*, **11**, 1553 (2001).

[12] (a) X.B. Cui, J.Q. Xu, Y.H. Sun, Y. Li, L. Ye, G.Y. Yang. *Inorg. Chem. Commu.*, **7**, 58 (2004); (b) S.T. Zheng, J. Zhang, G.Y. Yang. *Eur. J. Inorg. Chem.*, 2004 (2004); (c) S.T. Zheng, J. Zhang, G.Y. Yang. *J. Mol. Struct.*, **752**, 25 (2005).

[13] Y.G. Li, G.J.H. De, M. Yuan, E.B. Wang, R.D. Huang, C.W. Hu, N.H. Hu, H.Q. Jia. *J. Chem. Soc., Dalton Trans.*, 331 (2003).

[14] Y. Hou, S.T. Wang, E.H. Shen, D.R. Xiao, E.B. Wang, Y.G. Li, L. Xu, C.W. Hu. *J. Mol. Struct.*, **689**, 81 (2004).

[15] (a) G.M. Sheldrick. *SHELXS 97, Program for Crystal Structure Solution*, University of Göttingen, Germany (1997); (b) G.M. Sheldrick. *SHELXL 97, Program for Crystal Structure Refinement*, University of Göttingen (1997).

[16] D.K. Walanda, R.C. Burns, G.A. Lawrance, E.I. von Nagy-Felsobuki. *Inorg. Chim Acta*, **305**, 118 (2000).

[17] L. Bouhedja, N. Steunou, J. Maquet, J. Livage. *J. Solid State Chem.*, **162**, 315 (2001).

[18] (a) A. Müller, M. Renk, R. Rohlfing, E. Krickmeyer, J. Döring. *Angew. Chem., Int. Ed. Engl.*, **29**, 926 (1990); (b) A. Müller, J. Döring. *Z. Anorg. Allg. Chem.*, **595**, 251 (1991); (c) G.H. Huan, M.A. Greaney, A.J. Jacobson. *J. Chem. Soc., Chem. Commun.*, **4**, 260 (1991).

[19] D. Brown, D. Altermatt. *Acta Cryst.*, **B41**, 244 (1985).